

# Sizing of inhomogeneous particles by a differential laser Doppler anemometer

J Rheims<sup>†</sup>, T Wriedt<sup>‡</sup> and K Bauckhage<sup>†</sup>

<sup>†</sup> Universität Bremen, VT / FB 4, Postfach 330 440, 28334 Bremen, Germany

<sup>‡</sup> Stiftung Institut für Werkstofftechnik, Badgasteiner Strasse 3, 28359 Bremen, Germany

Received 25 August 1998, in final form and accepted for publication 16 November 1998

**Abstract.** A particle moving across the interference pattern of two intersecting laser beams scatters the incident light with a temporal variation that enables the calculation of particle velocity. This idea was realized in laser Doppler anemometry (LDA). By recording the light scattering pattern with a fast line scan sensor, the spatial modulation of the signal is also detected. This yields, in addition to particle velocity, information about the size and morphology of the particle.

This is the working principle of a new measuring device presented in this paper, the differential laser Doppler anemometer (DLDA). The theoretical background, principle of data evaluation and first experimental results of water and emulsion droplets and of glass beads are described.

**Keywords:** particle size, particle velocity, particle composition, surface structure, laser Doppler anemometer, CCD line scan sensor, spectrum analysis, picture analysis, particle characterization, two-phase flows

## 1. Introduction

It is well known that the light scattering patterns of not completely absorbing particles show spatial variations which are related to the size, optical properties and the morphology of the scattering object [1]. According to the principles of geometrical optics, this pattern is caused by the interference of beams that have been reflected at the particle surface and refracted into the particle in different orders. To determine particle size, the range of forward scattering past the region dominated by diffraction is of special interest. In this range, the scattering pattern is dominated by the interference of two orders only: reflected light and first-order refracted light [2].

This principle has been utilized to determine the properties of homogeneous, transparent droplets, for example by Wyatt [3], Davis [4], Ray [5] and their co-workers. They determined particle size and refractive index by comparing the measured light scattering patterns with results from Mie-computations. Particle size and refractive index were varied in the course of computations, which were terminated after an optimum agreement between the measured and computed scattering patterns had been obtained. This inversion solution to Mie-theory gives very accurate results, but it is very time-consuming and not suitable for on-line measurements. As computational demands of Mie-theory increase drastically with particle size, none of the cited references give results of particles with a diameter exceeding approximately 50  $\mu\text{m}$ .

To simplify computational demands and to make the method applicable to larger particles, signal evaluation can be

reduced from evaluating the angular course of the scattered signal to determining only the spatial distance of consecutive minima or maxima, that is, the number of oscillations in the observed angular range. This method was first suggested by Davis and Ravindran [4] and experimentally verified by König *et al* [6] and Hesselbacher *et al* [7]. Using a charge coupled device (CCD) line scan sensor with 1024 pixels, the latter two research groups measured the light scattered by monosized propanol-2-droplets with a diameter of 50  $\mu\text{m}$ , respectively 90  $\mu\text{m}$ , and claimed an accuracy of  $\pm 1\%$ .

Min and Gomez [8] replaced the method of counting the number of oscillations per angular range by determining the spatial frequency of the signal. This was accomplished by transforming the spatially resolved signal into the frequency domain by a fast Fourier transform (FFT). The FFT is followed by the determination of the dominant spectral line, which is related to the spatial frequency dominating the signal and which increases with particle size. Measuring monosized heptane droplets with a diameter of 75  $\mu\text{m}$  and using a photodiode array with 512 pixels, they obtained an accuracy of  $\pm 0.5\%$ .

Min and Gomez compared theoretical results from plane wave Mie-theory [9] to results obtained with the generalized Lorenz-Mie theory (GLMT), which is based on a Gaussian beam representation of the incident laser light [10]. They demonstrated that the Gaussian beam profile neither affects the pattern of scattered light nor the particle size derived from this datum. The same result was obtained experimentally by Hesselbacher *et al* [7].

To obtain the claimed accuracy of  $\pm 0.5\%$ , Min and Gomez evaluated a second feature of the scattered light, the phase of the dominant frequency or, in other words, the position of this oscillation within the observed angular range. This imposes two major disadvantages on their method. First, to ensure an accurate measure of the phase, the sensor must be positioned with high accuracy in the field of scattered light. Second, the oscillations must be resolved on a high number of pixels. This is due to the fact that they do not take advantage of interpolation techniques so that their evaluation method requires a high number of data points per oscillation. As the number of oscillations is proportional to particle size, this reduces the dynamic range of the method.

Another approach to determine particle size and velocity stems from laser Doppler anemometry. Farmer used the modulation depth of the LDA-signal to determine particle size [11]. Later, Stümke hinted at the limitations of this approach, especially in application to solid particles [12], where the modulation depth of the scattered signal is diminished by surface defects. Although even Durst and Zaré pointed out the possibility of using the spatial modulation of the scattered light for particle sizing [13], the use of this method was abandoned with the advent of phase Doppler anemometry (PDA) [14].

Independently from Min and Gomez, Rheims *et al* suggested a similar method to determine the core and shell size of coated particles [15]. The major difference to the method of Min and Gomez is, besides the different fields of application, that Rheims *et al* improved the accuracy of size determination by an interpolation technique instead of the phase of the dominant frequency. This measure reduced the demands on an accurate positioning of the sensor. Furthermore, their implementation in an LDA set-up results in a temporal variation of the signal, which permits the calculation of particle velocity. In the following, a method was developed where the single detector of an LDA system was replaced by a CCD line scan sensor with 256 pixels. Instead of one signal, 256 signals were detected so that the scattered light was captured with high spatial resolution. Therefore, we suggest the term ‘differential laser Doppler anemometry’ (DLDA) for this device. A profound description of this method can be found in the PhD thesis of Rheims [16].

The experimental set-up and optimization procedures are depicted in the next two sections, followed by the description of signal evaluation techniques of DLDA. In section 5, selected experimental results are given for water and suspension droplets, and for solid particles with intact and defect surface. These results prove that the DLDA can be used to measure the size and velocity of such particles with high precision.

## 2. Experimental set-up

The sending system, figure 1, is identical to the systems used in LDA, except that a high laser power of up to 3.5 W is mandatory due to the smaller detector units. For this reason, a frequency-doubled Nd:YVO<sub>4</sub> laser emitting green light at  $\lambda = 532$  nm was used<sup>†</sup>. The receiving system consisted

<sup>†</sup> Spectra Physics Lasers 1996 Millennia, Diode-pumped, Nd:YVO<sub>4</sub> CW Laser: User’s Manual (Mountain View, USA).

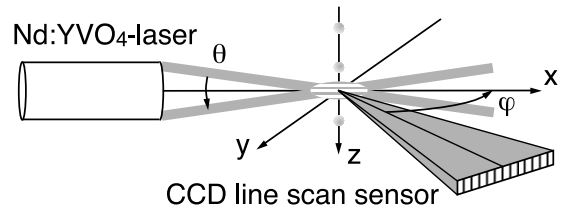


Figure 1. The optical geometry of the differential LDA (DLDA).

of a CCD line scan sensor with 256 pixels<sup>‡</sup>, arranged in the  $x,y$ -plane which is the plane of symmetry of the optical set-up. The sensor can also be arranged perpendicularly to the  $x,y$ -plane, which requires a different approach to signal evaluation and results in another experimental technique. This method, the differential phase Doppler anemometry (DPDA), is described elsewhere [16–18].

The CCD-sensor constantly delivers data to the digitization board with a maximum line frequency of 98 kHz. The data are digitized to 8 bit corresponding to 256 grey levels and then transmitted to a PC. If the grey levels are beyond a threshold value this is interpreted as burst signal, which is evaluated according to section 4. Stuht [18] gives a detailed description of the hard- and software used for data acquisition and evaluation.

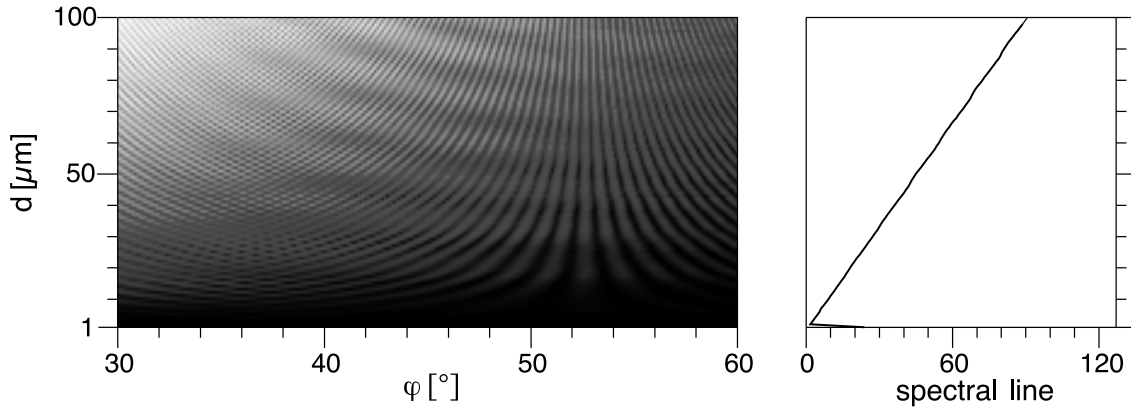
## 3. Optimization procedure

### 3.1. Particle size

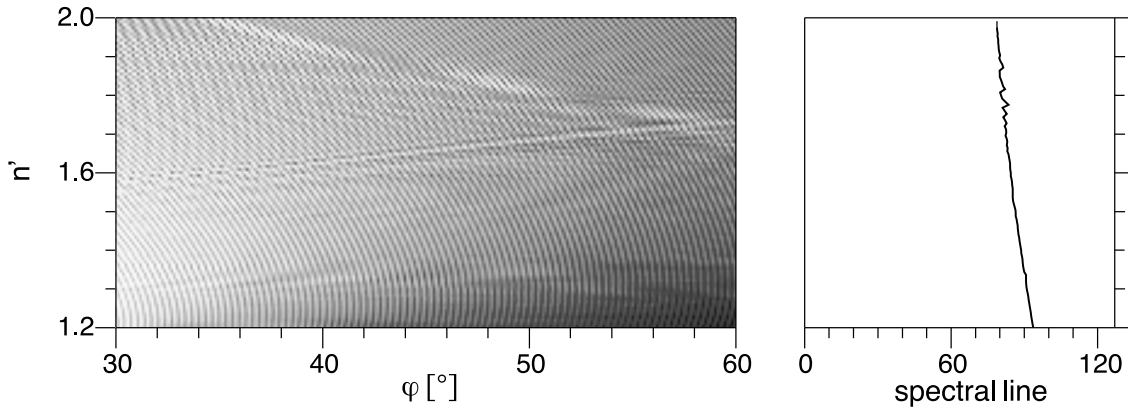
In the following, optimization of the experimental set-up is depicted for water droplets in the size range between 1 and 100  $\mu\text{m}$ . Calculations are based on Mie-theory and were performed with the PC-program *Scatap* [19]. For the sake of brevity, the following presumptions shall be introduced. The laser emits light at a wavelength  $\lambda$  of 532 nm with perpendicular polarization, i.e. the laser beams are polarized perpendicularly to the  $x,y$ -plane. The half-beam crossing angle is  $\theta/2 = 0.3^\circ$ , the resulting interference fringe spacing  $\Delta x$  is 51  $\mu\text{m}$ . The line scan sensor covers an off-axis angle range  $\varphi$  from 30 to 60°. The sensor is arranged in this position for two reasons: the intensity of scattered light is at maximum, and the scattered light shows distinct modulations, which show a clear variation with particle size. This modulation results from the interference of light reflected at the particle surface with rays of first-order refraction. Signal modulation is better for perpendicular polarization, because in this case the ratio of refracted to reflected light is higher than for parallel polarization [2]. At  $\lambda = 532$  nm, the refractive index of water is  $n = 1.33 - i0.0$  [2].

Figure 2 shows on the left the composition of scattered light computed for this experimental set-up. The abscissa shows the used off-axis angle range  $\varphi$ , varying from 30° to 60°. Calculations were performed for droplet diameters between 1 to 100  $\mu\text{m}$ , which are depicted on the ordinate axis. The increase of the intensity of scattered light and, even more important, of the number of oscillations with particle size can be clearly seen.

<sup>‡</sup> Dalsa Inc. 1994 CI-Cx Camera User’s Manual (Waterloo, Canada).



**Figure 2.** Composition of light scattering patterns (left) and frequency spectra (right) computed for water droplets.



**Figure 3.** Composition of light scattering patterns (left) and frequency spectra (right) computed for refractive indices  $n'$  between 1.2 and 2.0, no absorption.

In the next step, the light scattering pattern of each particle size was subjected to a frequency analysis. Traditionally, this is accomplished by a fast Fourier transform (FFT). In the case of DLDA, an estimation method, the autoregressive method (AR) or maximum entropy method (MEM), was employed [20–22]. This method is based upon the assumption that in every signal there is white, uncorrelated noise superimposed upon the spectrum. Using the MEM, the parameters of the estimation routines are adapted until an optimum agreement between generated and original data sets is obtained. With these parameters, the frequency spectrum of the signal can be determined.

The MEM was preferred to the FFT because it showed a better aptitude in identifying the dominant features of the signal. This was especially important when investigating inhomogeneous or non-spherical particles. Furthermore, the MEM algorithms were faster than the FFT routines [16]. Both were taken from the textbook written by Press *et al* [22].

Figure 2 displays on the right-hand side the variation of the magnitude of the dominant or characteristic spectral line with particle size. The spectral line 0 stands for the constant part of the signal; at the spectral line 127, the highest number of oscillations describable with this set-up, 127, can be identified. It can be clearly seen that this parameter, the number of oscillations  $n_{osc}$  in the observed angular range, is linearly related to particle size for diameters above  $2 \mu\text{m}$ . A

regression analysis applied to this relationship yields to

$$d/\mu\text{m} = 1.11n_{osc} - 0.04. \quad (1)$$

### 3.2. Particle refractive index

As the refractive index  $n'$  of the dispersed material is not always precisely known, it is also important to know the influence of this parameter on the composition of the DLDA signal. Figure 3 gives on the left the patterns of scattered light with the real part of the refractive index varying from 1.2 to 2.0. The imaginary part was set to 0 (completely transparent), particle diameter was kept constant at  $100 \mu\text{m}$ .

On the right of figure 3, the belonging frequency spectra are shown. The number of oscillations decreases slightly with increasing refractive index, but the influence of this parameter on the light scattering pattern is rather small. If, for example, the refractive index  $n'$  varies by  $\pm 0.02$ , this leads to an error in size determination of only  $\pm 0.4\%$ .

### 4. Signal evaluation

The computational results presented in the previous section showed the light scattering patterns of particles in the centre of the interference volume. As the sensor also detects light when the particle is out of this position, a DLDA burst is formed as is depicted for a water droplet in the left part of

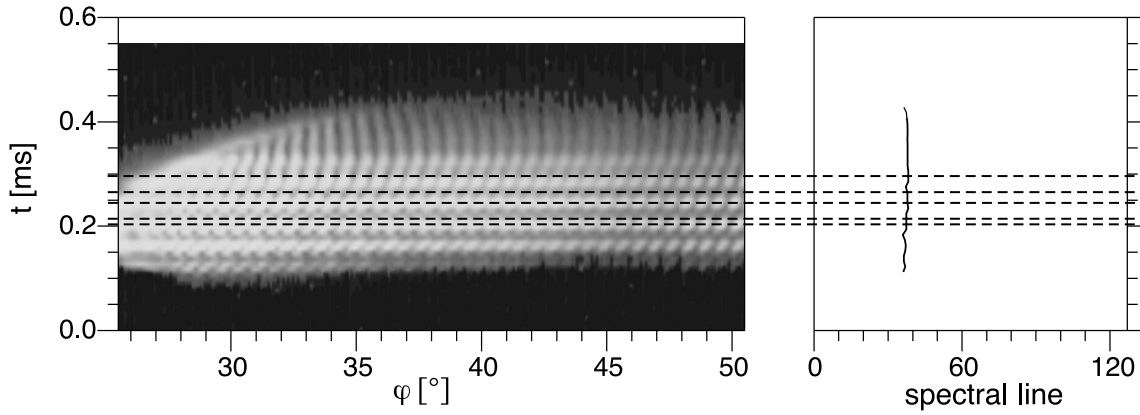


Figure 4. DLDA-burst and spatial frequency spectrum of a water droplet.

figure 4. The abscissa shows the spatial variation of the burst in the off-axis angle range between  $25.5^\circ \leq \varphi \leq 50.5^\circ$ . It bears a pattern caused by the aforementioned interference of reflected and first-order refracted light, which is related to particle size. The temporal variation of the signal, which lasts 0.55 ms including pre- and post-trigger, is caused by the projection of the interference fringe pattern onto the sensor. With knowledge of the interference fringe spacing and the line frequency of the CCD sensor, this variation permits the computation of particle velocity.

Generally, the evaluation of such signals can be performed in two different ways. Either it is based on the entire signal, or on selected parts of the burst, for example the lines of highest intensity in the temporal and spatial dimensions. Using the first alternative, detailed information can be obtained from the scattering process and thus from the particle passing the interference volume. The disadvantage is the high computational time required. The other option, evaluating just one line from the burst, is very fast, but rather error prone.

Therefore, as a compromise and because only few lines of the DLDA burst bear high intensity, the five brightest lines in each dimension, temporal and spatial, were selected for evaluation. These lines are marked in the burst on the left of figure 4 for the angular scattering pattern by the broken lines. The maximum entropy method was applied to the five spectra of each dimension, followed by averaging over these lines. Thereby, an average spectral line was obtained for the temporal and spatial variation of the signal. On the right-hand side of figure 4, the result for this kind of size determination is shown: the straight line shows the course of the dominating spatial frequency over time. As surface tension forces the water droplets into a perfect, spherical shape, neither particle surface nor the scattered signal are distorted so that the dominating spatial frequency remains fixed at an interpolated spectral line of 37.6. With knowledge of the relationship between the number of oscillations in the observed angular range and particle size,

$$d/\mu\text{m} = 142n_{osc} - 0.40 \quad (2)$$

the diameter of this droplet is calculated to be  $53 \mu\text{m}$ .

## 5. Experimental results

### 5.1. Water droplets

In the first step, the differential LDA was applied to water droplets. They were produced with high uniformity by a piezoelectric droplet generator [23]. The smallest water droplets measured with DLDA had a diameter of  $25 \mu\text{m}$ , the largest,  $73 \mu\text{m}$ . The results from DLDA were compared to PDA measurements, and no significant difference could be found [16]. The burst depicted in figure 4 was obtained during these measurements.

### 5.2. Suspension droplets

Suspension or emulsion droplets are also spherical, but they contain small inclusions (with a size comparable to the illumination wavelength) which distort the scattering process. Thereby, the diameter of the carrier droplet cannot be determined as precisely as for homogeneous droplets composed of one transparent liquid only, and new approaches to particle sizing had to be developed. Mitschke *et al* [24], for example, extended the application range of PDA in two different ways: first, by a mathematical method correcting the measured size distribution; second, by using a laser wavelength in the infrared ( $\lambda = 1312 \text{ nm}$ ), where the effects of the inclusions on the scattering process are reduced.

In this paper, a third option, a multiple measurement of the scattered light by DLDA, shall be introduced. The results were compared with PDA measurements. The diameter  $d_z$  of the interference volume used in DLDA and PDA measurements was fixed at  $550 \mu\text{m}$  with an interference fringe spacing  $\Delta_x$  of  $51 \mu\text{m}$ . The CCD sensor was operated at the maximum frequency of 98 kHz and detected the scattered light between  $25.5^\circ \leq \varphi \leq 50.5^\circ$ , at a range of  $d\varphi = 0.1^\circ$  per pixel. The centres of the PDA detectors were arranged at the off-axis angle  $\varphi = 52^\circ$  and the elevation angle  $\Psi = \pm 3.1^\circ$ . The angles covered by the rectangular PDA apertures were  $d\varphi = 9.2^\circ$  and  $d\Psi = 1.2^\circ$ .

To ensure reproducible experimental conditions, a method was developed to create such solid inhomogeneities [25]. An electron microscopic picture of polystyrene (PS) particles produced by this method is shown in figure 5. Their mean diameter is  $440 \text{ nm}$  with a standard deviation

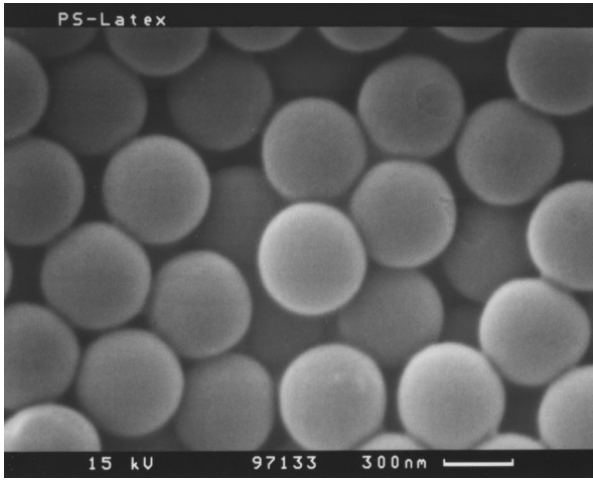


**Figure 5.** REM photo of monodispersed polystyrene particles.

**Table 1.** Diameters of monodispersed water and suspension droplets. DLDA and PDA data are based on 500 measurements.

	DLDA	PDA
	$d$ ( $\mu\text{m}$ )	$d$ ( $\mu\text{m}$ )
Water	$52.8 \pm 0.2$	$53.3 \pm 1.8$
0.25% latex	$53.1 \pm 1.1$	$52.6 \pm 7.0$
0.50% latex	$50.5 \pm 1.4$	$48.3 \pm 8.5$

**Table 2.** Velocities of monodispersed water and suspension droplets. DLDA and PDA data are based on 500 measurements.

	DLDA	PDA
	$v$ ( $\text{m s}^{-1}$ )	$v$ ( $\text{m s}^{-1}$ )
Water	$1.22 \pm 0.02$	$1.25 \pm 0.00$
0.25% latex	$1.23 \pm 0.06$	$1.15 \pm 0.01$
0.50% latex	$(1.85 \pm 0.24)$	$1.19 \pm 0.02$

**Table 3.** Diameters of two glass beads measured with DLDA and PDA. DLDA and PDA data are based on 400 measurements of the same particle.

	DLDA	PDA	References
	$d$ ( $\mu\text{m}$ )	$d$ ( $\mu\text{m}$ )	$d$ ( $\mu\text{m}$ )
Particle 1	$515.8 \pm 1.3$	$483.2 \pm 20.3$	$517 \pm 3$
Particle 2	$511.1 \pm 3.5$	$435.4 \pm 23.0$	$500 \pm 3$

**Table 4.** Velocities of two glass beads measured with DLDA and PDA. DLDA and PDA data are based on 400 measurements of the same particle.

	DLDA	PDA	References
	$v$ ( $\text{m s}^{-1}$ )	$v$ ( $\text{m s}^{-1}$ )	$v$ ( $\text{m s}^{-1}$ )
Particle 1	$0.41 \pm 0.00$	$0.40 \pm 0.01$	$0.41 \pm 0.03$
Particle 2	$0.45 \pm 0.06$	$0.45 \pm 0.01$	$0.45 \pm 0.03$

of  $\pm 10$  nm. They are transparent and have a refractive index  $n'$  of 1.60 at  $\lambda = 532$  nm [26]. If such particles are diluted in water with a mass concentration of only 0.5%, and if this latex suspension is dispensed and forms carrier droplets with a diameter of  $50 \mu\text{m}$ , each droplet contains some 10 000

PS particles which affect the light scattering process and the accuracy of size determination of the carrier droplet.

The effect of the inhomogeneities on light scattering can be easily identified by comparing the DLDA burst depicted in figure 6 with figure 4. First, it can be seen that the intensity of light scattered by the suspension droplet has decreased. Second, the light scattering pattern is blurred and much less clearly modulated than in the case of the water droplet. This effect of the inhomogeneities can also be seen in the spatial frequency pattern, where strong oscillations in the course of the dominant spectral line occur. The diameter of the droplet, however, is still determined with good accuracy, as the following evaluation will show.

To obtain a comparable database, three different liquids were investigated by DLDA: pure water, water with 0.25 mass% latex, and water with 0.50 mass% latex. Results were compared to PDA measurements; furthermore, the reference diameter of the droplets,  $53 \mu\text{m}$ , was determined by a microscope.

Table 1 shows the measured particle diameters. In each case, the mean diameter and the standard deviation were determined based on 500 measured droplets. For water droplets, there is no significant difference between the mean diameters measured by the microscope, DLDA or PDA. The standard deviation of size measurements is extraordinary low for DLDA and reasonably good for PDA. With increasing latex concentration, the measured standard deviation increases. For the highest concentration that could be dispensed with the droplet generator, 0.5%, it is  $\pm 8.5 \mu\text{m}$  or  $\pm 18\%$  for PDA. In the case of DLDA, it increases to only  $\pm 1.4 \mu\text{m}$  or  $\pm 3\%$  so that is even lower than in the case of PDA measurements with pure water.

The measured velocities, table 2, are always close together and are measured with low standard deviations. The only exception is the DLDA measurement with the highest latex concentration. In this case, the measured velocity deviates by approximately 50% from the velocities measured with the other particle types. The probable reason is that due to the relatively low maximum line frequency of the sensor, 98 kHz, signal duration is too short to get a reasonable database for velocity determination. This error does not occur in PDA, because in this case signals were captured at 500 kHz.

### 5.3. Glass beads

To further verify the DLDA, transparent glass spheres (Schott, type LaSf 35,  $n' = 2.04$  at  $\lambda = 532$  nm [27]) were attached to thin wires ( $100 \mu\text{m}$  diameter), mounted on to the shaft of a rotating electric motor and thus moved through the measuring volume repeatedly. The particle reference diameter was determined under the microscope and is given in table 3. It was determined by use of an image analysis system, the standard deviation given is an estimate of random and systematic errors occurring in the course of calibration. The reference velocity was calculated by the speed of the motor and the circumference of the particle trajectory. It can be found in table 4.

The CCD sensor was arranged in the off-axis angle range  $19^\circ \leq \varphi \leq 25^\circ$ , the range observed by each pixel was  $d\varphi = 0.02^\circ$ . The correlation between the number

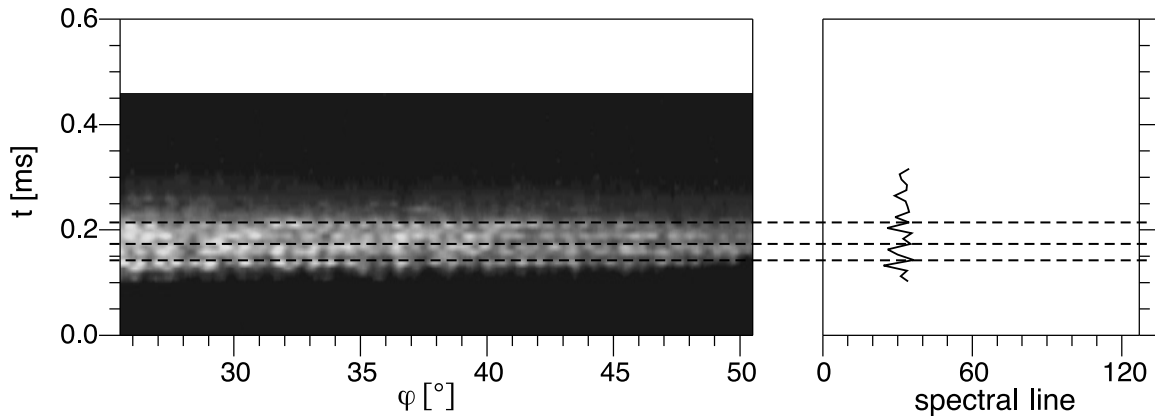


**Figure 6.** DLDA-burst and spatial frequency spectrum of a water droplet containing 0.5 mass% polystyrene.



**Figure 7.** Photo of glass bead 1 with intact surface.

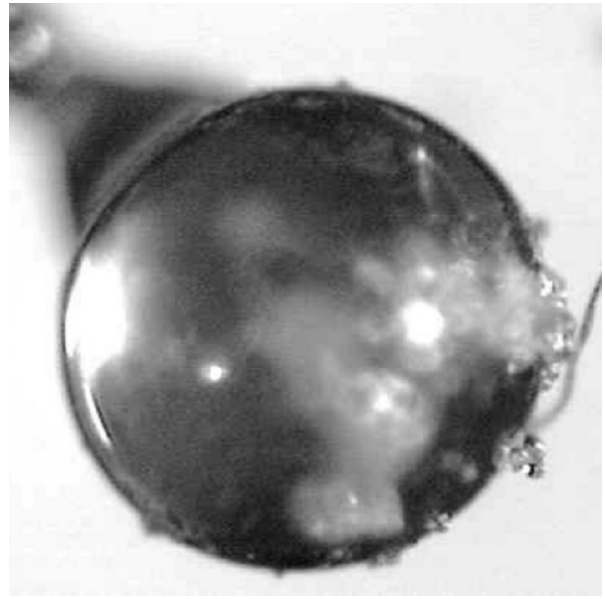


**Figure 8.** Photo of glass bead 2 with defect surface.

of oscillations in the observed angular range and particle diameter was calculated to be

$$d/\mu\text{m} = 7.56n_{osc} - 1.43. \quad (3)$$

The PDA measurements were performed at an off-axis angle  $\varphi$  of  $52^\circ$  and with an elevation angle  $\Psi$  of  $\pm 3.1^\circ$ ; the detectors covered the same angle range as before:  $d\varphi = 9.2^\circ$ ,  $d\varphi = 1.2^\circ$ . In both cases, the sending system was arranged as described in section 3. The interference volume had a diameter  $d_z$  of 2.2 mm.

Prior to the complete experimental results, two selected single results shall be shown. They were obtained with two glass spheres of different surface qualities. Figure 7 shows a photo of glass sphere 1 with apparently intact surface, figure 8, particle 2 with poor surface quality.

The DLDA signal of particle 1, figure 9, shows a distinct modulation in both the temporal and spatial dimension of the burst. The variation in the dominating spectral line over time is insignificant, and particle size is determined to  $d = 513 \mu\text{m}$ . The reference diameter is  $517 \mu\text{m}$ .

The DLDA signal of particle 2, figure 10, is much less clearly modulated, and the distortions propagate into the spatial frequency spectrum. The measured particle size,  $d = 513 \mu\text{m}$ , is still close to reference data ( $d = 500 \mu\text{m}$ ).

Tables 3 and 4 show the results of 400 DLDA and PDA measurements of the same particle. Contrary to calibration, the standard deviation is now attributed to random errors occurring in the course of measurements only. For DLDA, a very good agreement with reference data and a very low standard deviation is obtained for both particles and for both parameters, particle size and particle velocity. In the case of PDA, only the velocity is determined correctly, but the measured particle diameters differ significantly from the reference values. This implies that the characteristic spectral line is determined correctly, but, due to the aforementioned defects on the particle surface and within the particle, the phase information is corrupted.

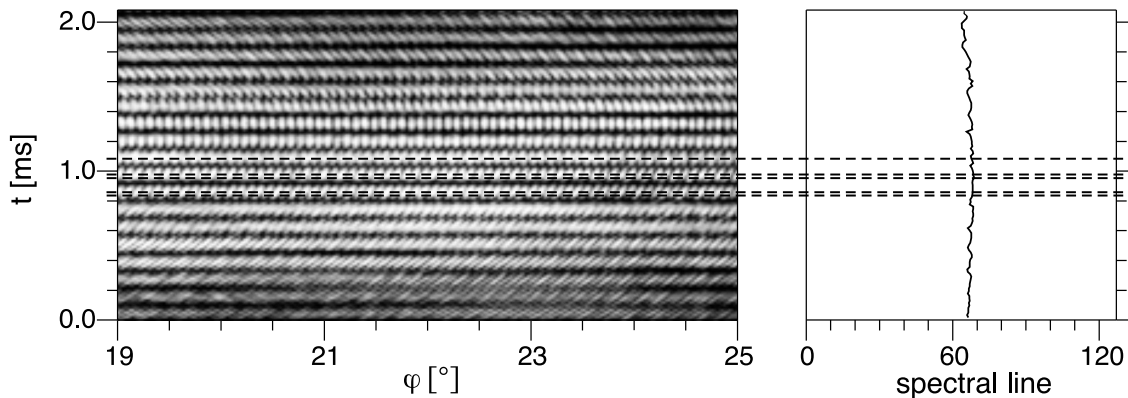


**Figure 9.** DLDA-burst and spatial frequency spectrum of glass bead 1 with intact surface.

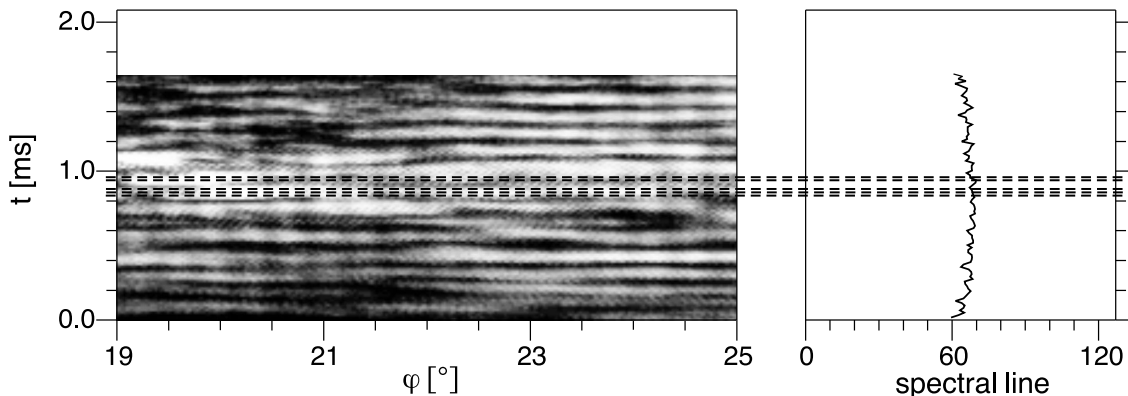


**Figure 10.** DLDA-burst and spatial frequency spectrum of glass bead 2 with defect surface.

## 6. Conclusions

Theoretical and experimental results presented in this paper demonstrate the availability of a new method for measuring particle size and velocity, the differential LDA or DLDA. Compared with PDA, the DLDA is not sensitive to Gaussian beam defects. Furthermore, it bears the potential of exact size determination even under severe conditions such as spheres with inhomogeneous composition or surface defects. DLDA measurements of such particles show much better results than with PDA. The smallest particles measured with DLDA so far, water droplets, had a diameter of  $25\ \mu\text{m}$ . From theoretical investigations, size measurements down to some  $2\ \mu\text{m}$  seem to be possible. There is no upper limit for particle size.

The maximum particle velocity that can be measured with CCD detectors currently is approximately  $10\ \text{m s}^{-1}$ . This clearly restricts the application range of CCD technology, but technical progress will certainly increase this limit.

Replacing the CCD line scan sensor by a photomultiplier device, the maximum velocity that can be measured by DLDA increases by about one order of magnitude. However, there are two disadvantages connected to this approach. First, a photomultiplier device requires a much more sophisticated signal transfer and processing hardware than a CCD device. Second, multichannel photomultipliers are much more expensive than CCD sensors.

Extensions of the DLDA to other types of particles are currently under investigation. Special interest is focused on

extracting further information from the DLDA burst. One option is the sizing of coated particles [16], another is to quantify inhomogeneities or surface defects by the course of the dominant spectral line over time.

## Acknowledgment

The authors gratefully acknowledge the support of this research project by the Deutsche Forschungsgemeinschaft (DFG) under grant No Wr 22/4-2.

## References

- [1] van de Hulst H C 1981 *Light Scattering by Small Particles* (New York: Dover)
- [2] Bergmann L and Schaefer C 1993 *Lehrbuch der Experimentalphysik, Band 3, Optik* ed H Niedrig (Berlin: de Gruyter & Co)
- [3] Wyatt P J 1980 Some chemical, physical, and optical properties of fly ash particles *Appl. Opt.* **19** 975–83
- [4] Davis E J and Ravindran P 1982 Single particle light scattering measurements using the electrodynamic balance *Aerosol Sci. Technol.* **1** 337–50
- [5] Ray A K, Johnson R D and Souyri A 1989 Dynamic behavior of single glycerol droplets in humid air streams *Langmuir* **5** 133–40
- [6] König G, Anders K and Frohn A 1986 A new light-scattering technique to measure the diameter of periodically generated moving droplets *J. Aerosol. Sci.* **17** 157–67

- [7] Hesselbacher K H, Anders K and Frohn A 1991 Experimental investigation of Gaussian beam effects on the accuracy of a droplet sizing method *Appl. Opt.* **30** 4930–5
- [8] Min S L and Gomez A 1996 High-resolution size measurement of single spherical particles with a fast Fourier transform of the angular scattering intensity *Appl. Opt.* **35** 4919–26
- [9] Mie G 1908 Beiträge zur optik trüber medien, speziell kolloidaler metallösungen *Ann. Phys., Lpz* **25** 377–452
- [10] Gouesbet G, Gréhan G and Maheu B 1991 Generalized Lorenz-Mie theory and applications to optical sizing *Combustion Measurements* ed N Chigier (New York: Hemisphere) pp 339–84
- [11] Farmer W M 1972 Measurement of particle size, number density and velocity using a laser interferometer *Appl. Opt.* **11** 2603–12
- [12] Stümke A 1979 Messung lokaler Häufigkeitsverteilungen von Partikelgeschwindigkeiten *Gas-Feststoff-Strömungen. Grundlegende Untersuchungen zum Einsatz eines Laser-Doppler-Velocimeter* (Düsseldorf: Fortschr. Ber. VDI) Reihe 3, Nr. 53
- [13] Durst F, Zaré M 1975 *Laser Doppler Measurements in Two-Phase Flows. Proc. LDA-Symp.* (Copenhagen: Nordita) pp 403–29
- [14] Hirleman E D 1996 History of development of the phase-doppler particle-sizing velocimeter *Part. Part. Syst. Charact.* **13** 59–67
- [15] Rheims J, Wriedt T and Bauckhage K 1996 *Bestimmung von Kern- und Gesamtdurchmesser schalenförmig aufgebauter, sphärischer Partikeln mittels des bei LDA erzeugten Streulichtmusters Proc. 5. Fachtagung Lasermethoden in der Strömungsmesstechnik* (Aachen: Verlag Shaker) pp 30.1–30.7
- [16] Rheims J 1998 *Partikelanalyse mittels differentieller Streulichtmessungen unter hoher räumlicher und zeitlicher Auflösung* (Düsseldorf: Fortschr. Ber. VDI) Reihe 8, Nr. 710
- [17] Rheims J, Wriedt T and Bauckhage K 1998 Working principle and experimental results of a differential phase-Doppler technique *Part. Part. Syst. Charact.* **15** 219–24
- [18] Stuht C 1997 Entwicklung eines Mehrprozessor-Bildverarbeitungssystems für die laseroptische Partikelmeßtechnik *Diploma thesis* FB 1, University of Bremen
- [19] *Scatap* is available at webpage <http://imperator.cip-iw1.uni-bremen.de/fg01/scatap.html>
- [20] Marple S L Jr 1987 *Digital Spectral Analysis with Applications* (Englewood Cliffs, NJ: Prentice-Hall)
- [21] Kaye S M and Marple S L Jr 1981 Spectrum analysis—a modern perspective *Proc. IEEE* **6** 1380–419
- [22] Press W H, Teukolsky S A, Vetterling W T and Flannery B P 1992 *Numerical Recipes in C* (Cambridge: Cambridge University Press)
- [23] Ulmke H and Wriedt T 1997 Piezoelektrischer Tropfengenerator zur Kalibrierung von Partikelzählern *Report VT/FB 4* Universität Bremen
- [24] Mitschke M, Wriedt T and Bauckhage K 1998 Standard PDA for measuring the size of inhomogeneous droplets *Meas. Sci. Technol.* **9** 193–205
- [25] Köser J 1997 Die Herstellung von Polystyrol-Latices *Report VT/FB 4* Universität Bremen
- [26] Kerker M 1969 *The Scattering of Light and other Electromagnetic Radiation* (New York: Academic)
- [27] Schott Glaswerke 1996 Optisches Glas Nr. 10000 D (catalogue) (Mainz: Schott Glaswerke)